Electronic Supplementary Material (ESI) for Journal of Materials Chemistry A.

Electronic Supplementary Information (ESI)

Recyclable, Weldable, Mechanically Durable, Programmable Liquid Metal-Elastomer Composites

Guokang Chen,[a, b, c] Xiaobo Deng,[a] Lifei Zhu,[a] Stephan Handschuh-Wang,[a] Tiansheng Gan,[a] Ben Wang,[a] Qixing Wu,[a] Hui Fang,[d] Nailin Ren,[c] and Xuechang Zhou*[a]

[a]College of Chemistry and Environmental Engineering, Shenzhen University, Shenzhen 518060, P. R. China. E-mail: xczhou@szu.edu.cn

[b]Key Laboratory of Optoelectronic Devices and Systems of Ministry of Education and Guangdong province, College of Optoelectronic Engineering, Shenzhen University, Shenzhen 518060, P. R. China

[c]College of Chemistry and Environmental Engineering, Hanshan Normal University, Chaozhou 521041, P.R. China

[d]Nanophotonics Research Center, Institute of Microscale Optoelectronics, Shenzhen University, Shenzhen 518060, P. R. China

*Corresponding author

(Xuechang Zhou*[a]) E-mail: xczhou@szu.edu.cn

Experimental Details

Characterization: Scanning electron microscopy (SEM) micrographs were recorded using FEI Nova NanoSEM450. To preserve the original cross-sectional morphology structure, all the samples were fractured in liquid nitrogen to obtain the cross-sectional SEM images. The hydrodynamic diameter of the LM droplets was measured by dynamic light scattering (Mastersizer 2000, Malvern instruments) utilizing a refractive index of 1.37. ^{1}H-NMR spectra were obtained on VNMRS 400 spectrometer. Deuterated dimethyl sulfoxide (DMSO) was used as the solvent. GPC was carried out against polystyrene standard with a Waters 515 instrument and DMF as eluent (solvent) at a flow rate of 1.0 ml/min. The X-ray diffraction (XRD) patterns were obtained using a Bruker D8 Advance X-ray diffractometer with Cu Kα radiation (k = 0.154 nm) at room temperature.

Gel fraction and swelling ratio of the composites: For swelling, small samples were immersed into DMF at room temperature for 48 h. The mass of the original sample (m_0), the mass of the swelled sample (m_1), and the mass of the dried sample (m_2) were measured. The gel fraction (G (%)) and the swelling ratio (S (%)) were calculated according to Equations 1 and 2, respectively:

$$G(\%) = \frac{m_2}{m_0} \times 100\% \tag{1}$$

$$S(\%) = \frac{m_1}{m_2} \times 100\% \tag{2}$$

Measurement of mechanical properties of the composites: For all stress-strain tensile tests, the samples (gauge width: 4 ± 0.5 mm, gauge length: 16 ± 2 mm, thickness: 0.4 ± 0.1 mm) were stretched uniaxial at a velocity of 5 mm/min until fracture with the tensile testing machine (CMT6103, SANS). For hysteresis tests at different tensile strains, the composite (30 vol%) was stretched to 20%, 40%, 60%, 80%, 100% strain, and immediately unloaded. The successive loading–unloading test was performed on the same sample. The Elastic modulus was determined from the slope of the stress-strain curve in the strain range between 0 ~ 10%. The fracture energy was calculated from $\Gamma=U(L_c)/a_0b_0$. Here, L_c is the length of the gel at fracture strain, $U(L_c)$ depicts the area beneath the force-displacement curve from the distance between 0 ~ L_c, and a_0 and b_0 are the width and thickness of the sample, respectively.

Fatigue tests were conducted by using computer-controlled moving stages (PSA050, Zolix). The resistance of the composites was measured by using a 4-point probe method by employing a Keithley 2400 sourcemeter.

The self-healing of the composite: Samples were completely separated by cutting with a clean razor blade. Subsequent the two fragments brought into contact, placed between two glass slides and fixed with clips. This setup was placed in an oven (120 ^{o}C) for 2 h and subsequently stored for 48 h at 60 ^{o}C. The apparent healing efficiency was determined by the electrical conductivity of the healed sample in comparison to the pristine sample.

Thermal-reprocessing of the composite: A representative sample was cut into small fragments and remolded through hot pressing (15 MPa) at 120 ^{o}C for 2 h and subsequently, storing for 48 h at 60 ^{o}C.

Solvent-reprocessing of the composite: A representative sample was dissolved in DMF at 120 ^{o}C (30 min). Subsequently, the solution was concentrated, cast into a Teflon mold and stored at 60 ^{o}C for 48 h.

Recycling of LM: The composite was immersed into DMF and heated to 120 ^{o}C. Subsequently, the solution was centrifuged and washed with DMF for several times to remove free macromolecules. Then, the precipitate was grinded in the presence of 0.6 M NaOH solution in a mortar. The LM droplets coalesced to form a sphere. Finally, the large LM droplet was readily separated in a petri dish and rinsed with deionized water.

Description of supporting videos

Video S1: Mechano-training of the composite (30 vol% and 50 vol% LM) to generate an electrical conductor. During the mechano-training process, the resistance of the composite decreased sharply.

Video S2: The extension performance of the spiral 3D conductive composite during mechanical stress.

Video S3: A LED bulb switched on by localized NIR induced welding of the conductive composite strips. Initially, no pressure is applied to the overlapping region of the strips. Thus, the circuit is not closed and the LED lamp did not emit light. After localized sintering with NIR and pressure, a closed circuit is obtained and the LED emitted light.

Video S4: The LM-elastomer composite could be used as the solder to weld the LED bulbs onto the composite-based circuit one by one with the assistance of the photothermal effect.

Supporting Figures

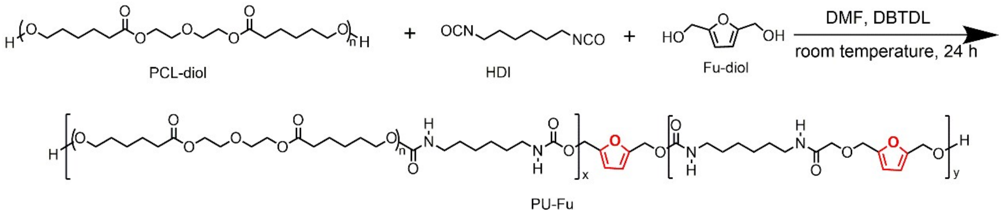

Scheme S1. Schematic of the chemical synthesis of the PU-Fu.

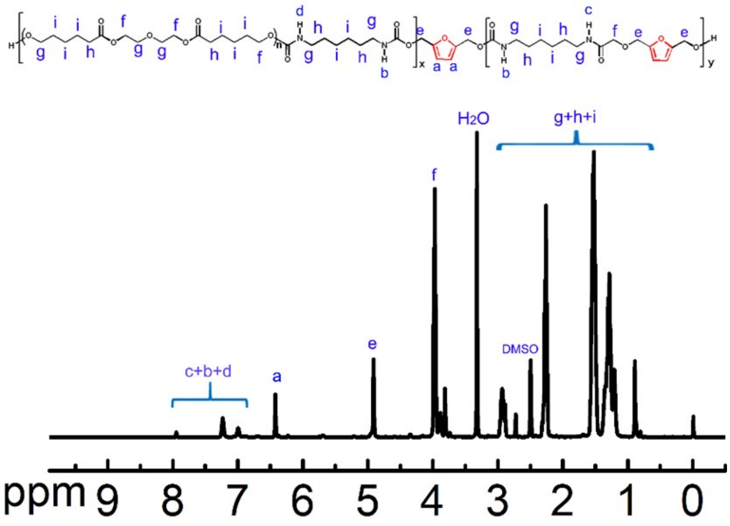

Fig. S1 ^{1}H-NMR spectra of PU-Fu.

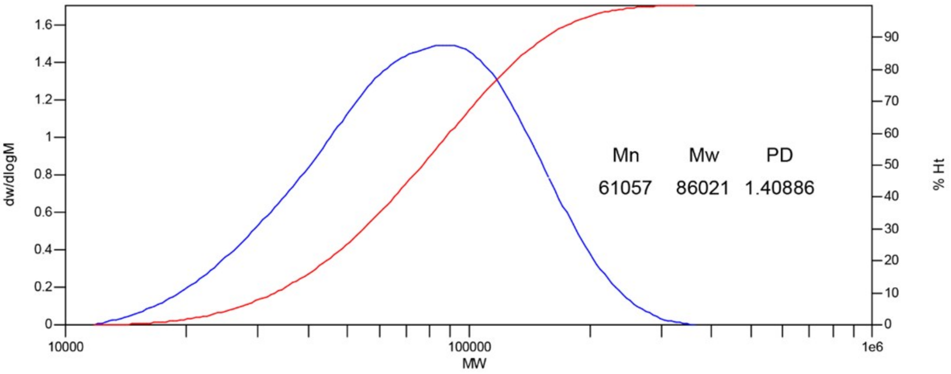

Fig. S2 The molecular weight distribution of the PU-Fu. DMF was used as the eluent and polystyrene as the standard.

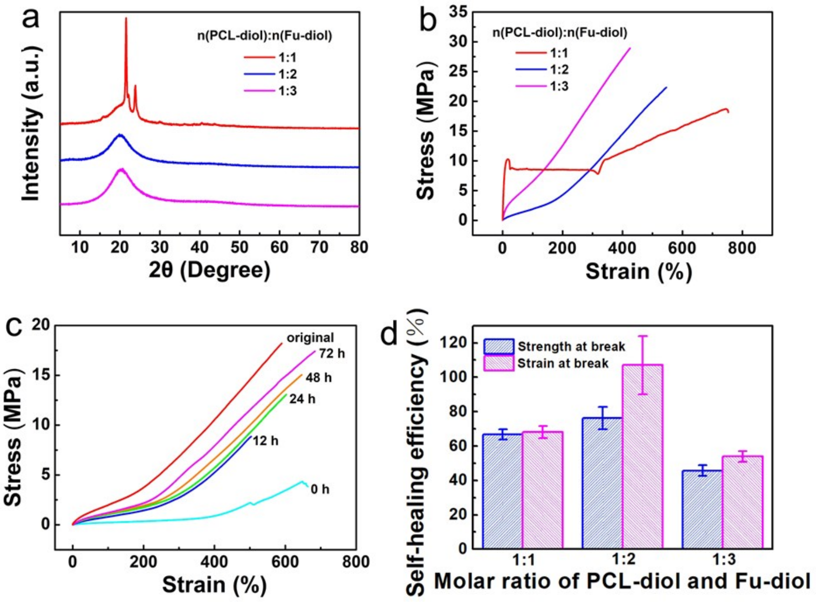

Fig. S3 a) XRD and b) representative stress versus strain curves for the as-made elastomers with different molar ratios of PCL-diol and Fu-diol. c) Stress versus strain curves for PUE12 at different healing times at 60 ^{o}C. d) Self-healing efficiency of the as-made elastomers.

By varying the molar ratio of PCL-diol and Fu-diol (1:1, 1:2, 1:3), three elastomers with different crosslinking densities can be obtained. These elastomers were named PUE11, PUE12, and PUE13, which represents the molar ratio of PCL-diol and Fu-diol (1:1, 1:2, 1:3), respectively. Crosslinking density has a huge influence on the properties of the elastomers. Obviously, high Fu-diol content results in high crosslinking density. As shown in Fig. S3a, the elastomer PUE11 exhibits crystalline behavior while PUE12 and PUE13 do not, which is in agreement with the mechanical behavior of these three elastomers (Fig. S3 b). Meanwhile, the elastomers exhibit good mechanical performance. Because of crystallization, PUE11 shows the highest elastic modulus up to 230 MPa while PUE12 shows a moderate modulus of about 4 MPa. Due to the properties of DA-based networks, the as-prepared elastomers exhibit excellent self-healing performance (Fig S3 c-d). These results demonstrate that PUE12 is the most suitable matrix for fabricating LM-elastomer composites due to its excellent self-healing performance, good stretchability and stress at break, and moderate module.

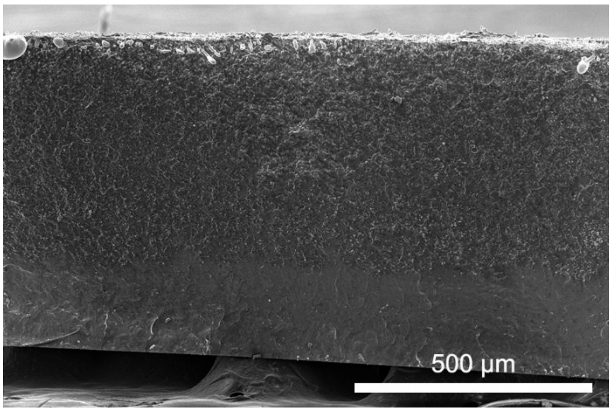

Fig. S4 The cross-sectional SEM micrograph of the composite (50 vol% LM) fabricated with a low concentration of prepolymer solution, demonstrating the sedimentation of LM droplets.

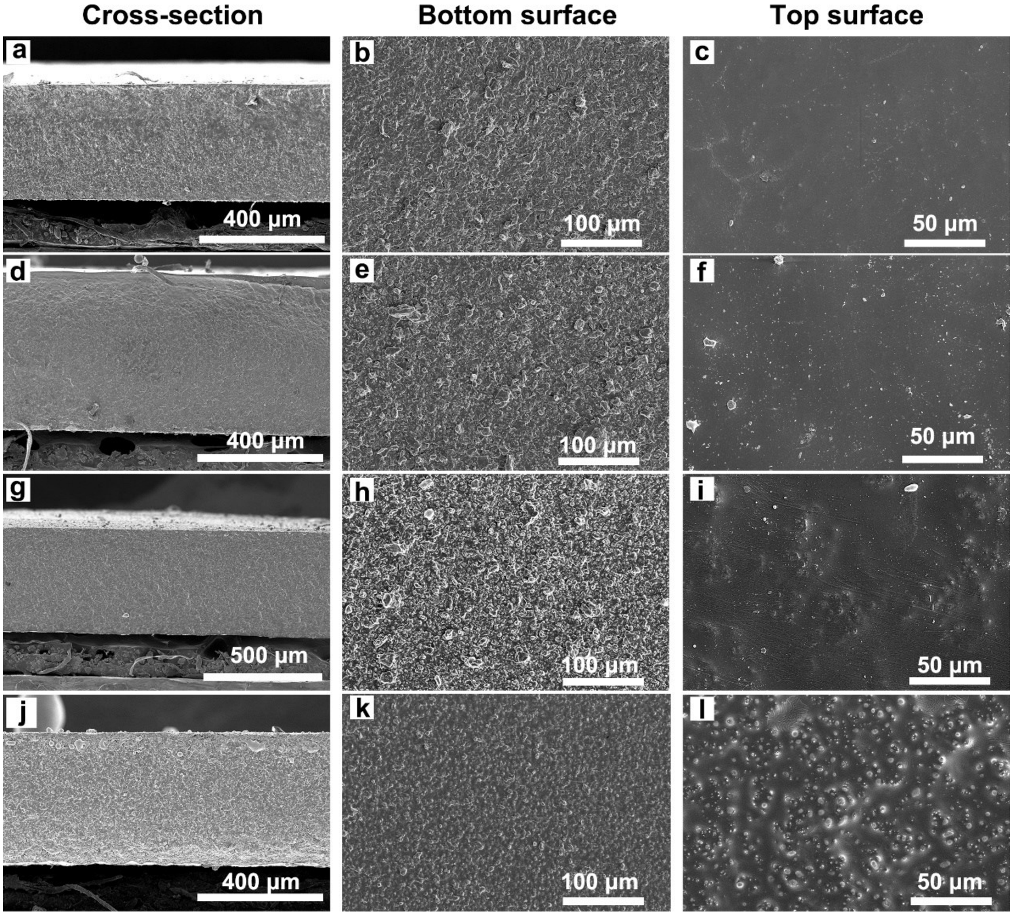

Fig. S5 SEM micrographs of LM-elastomer composites. The composites fabricated with LM volume ratio of (a~c) 20%, (d~f) 30%, (g~i) 40%, (j~l) 50%. The first column shows the cross-section of the composite; the second column shows the bottom surface and the third column shows the top surface of the composites.

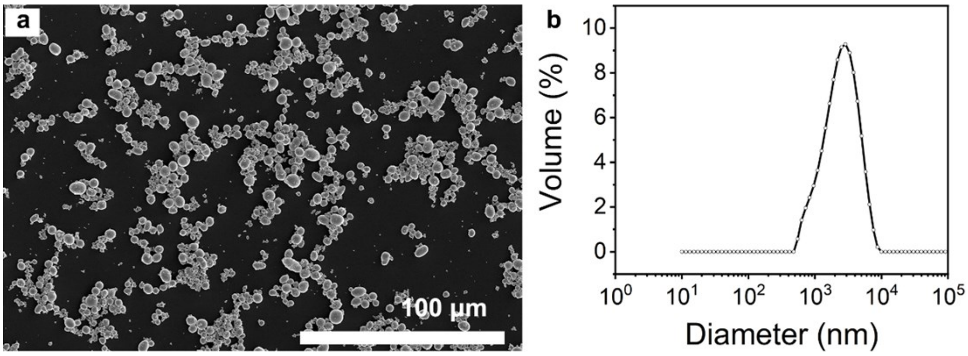

Fig. S6 a) SEM micrograph and b) size distribution (dynamic light scattering, DLS) of LM droplets fabricated by sonication in DMF for 10 min.

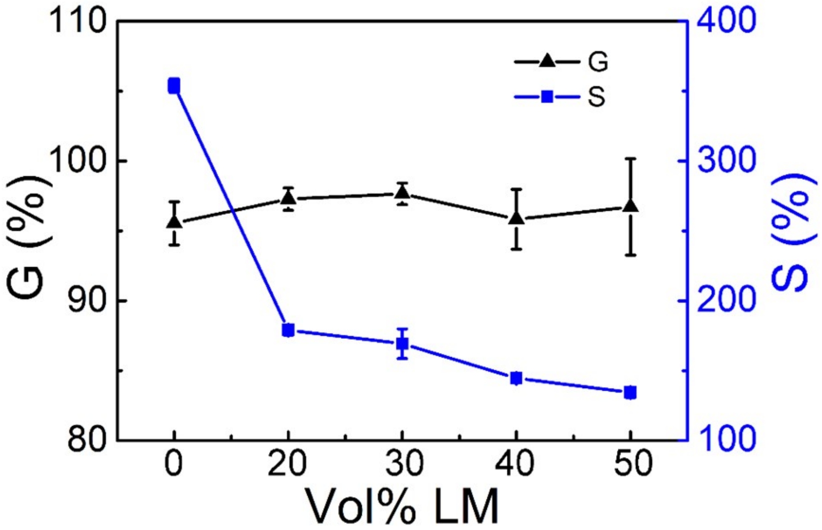

Fig. S7 The gel fraction and the swelling fraction of the composites. The result showed that the gel fractions of LM-elastomer composites were all larger than 95%, illustrating that a good covalent network was formed and the loading of LM had little influence on the gel fraction. The swelling ability of LM-elastomer composites in the solvent decreased upon an increase in the loading of LM. This was attributed to the fact that the LM droplets occupied the pores of the polymer network.

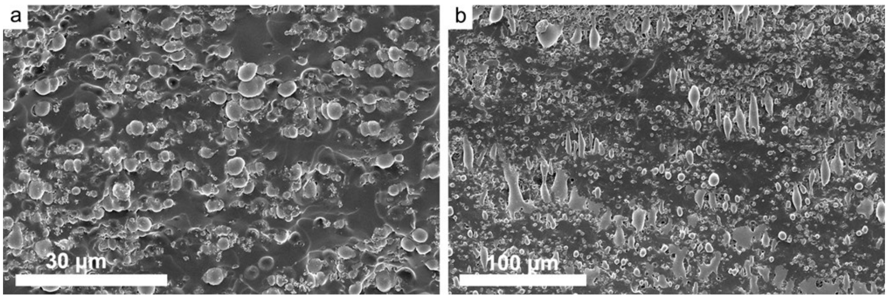

Fig. S8 Cross-sectional SEM micrographs of the composite (30 vol%) after 10 (a) and 100 (b) mechano-training cycles with an applied strain of 50%.

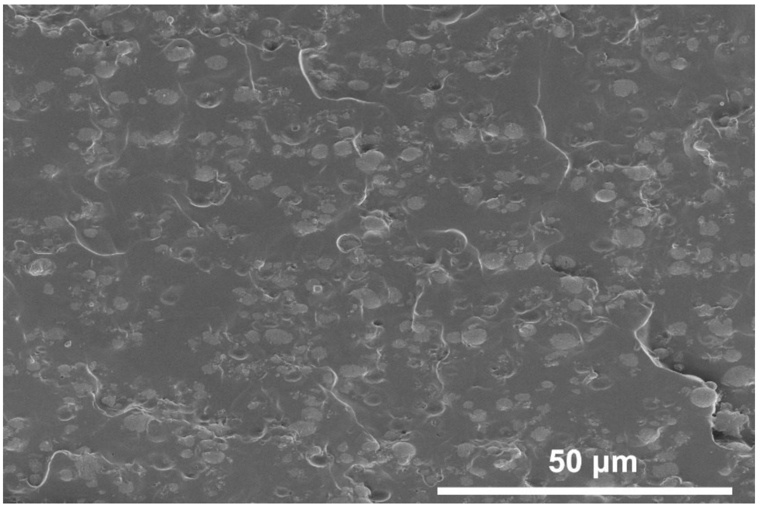

Fig. S9 Cross-sectional SEM micrograph of the composite (20 vol% LM) after mechano-training (500 cycles, tensile strain of 150%).

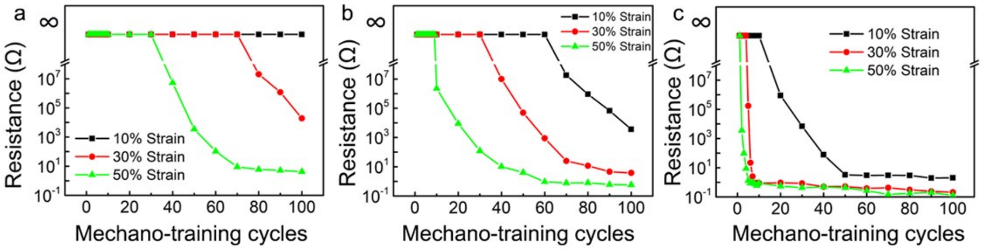

Fig. S10 Dependence of the measured resistance on the number of mechano-training cycles, vol% of incorporated LM (a: 30 vol%; b: 40 vol%; c: 50 vol%) and training strain. The experiment was performed at room temperature. The dimensions of the samples were 4.5 cm (length), 0.5 cm (width) and 0.04 cm (thickness). The symbol “∞” indicates the resistance beyond the measurement instrument.

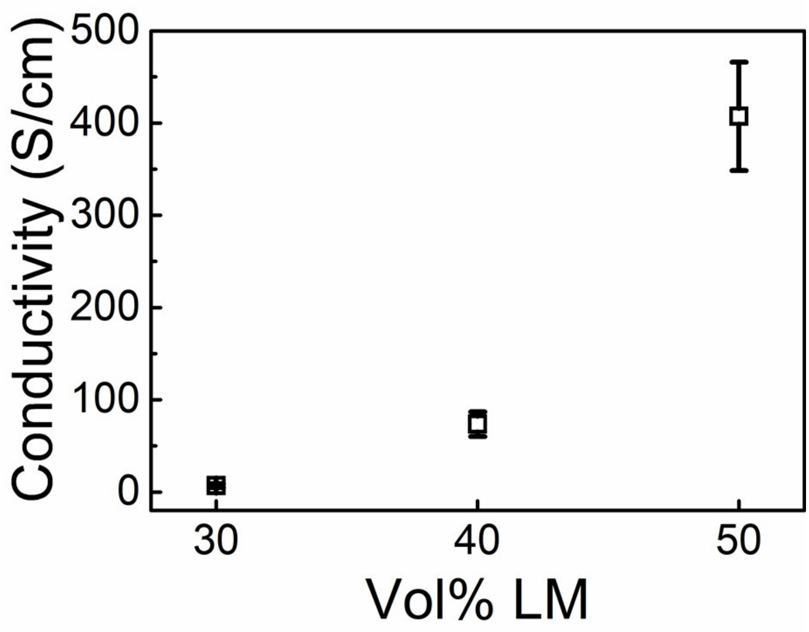

Fig. S11 Dependence of the electrical conductivity of the mechano-trained (50% tensile strain, 100 cycles) composites on the vol% of the LM in the composite.

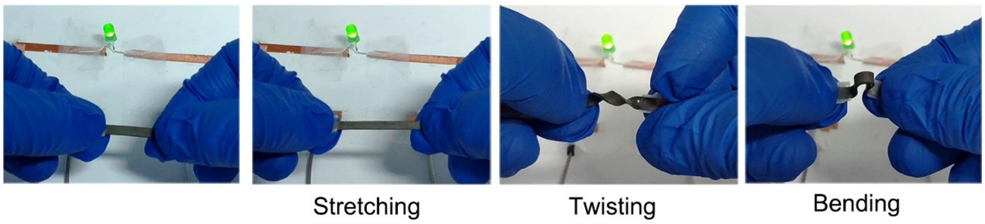

Fig. S12 Digital photographs showing the conductive (trained) composite, which was able to sustain various mechanical deformations (stretching, twisting, and bending).

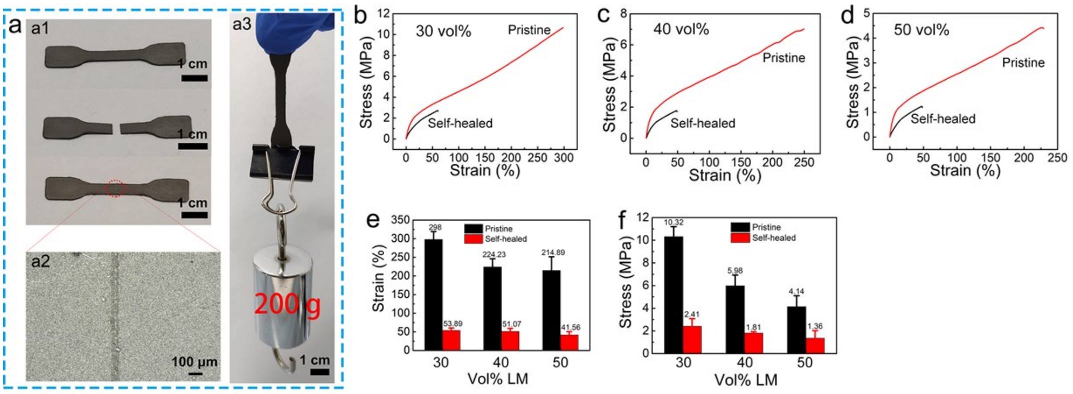

Fig. S13 Self-healing performance. (a1) Photographs of the composite before (top) and after cutting into two pieces (middle). The bottom picture shows a rejoined (healed) sample. (a2) Optical microscopy image of the healed region, showing no obvious cracks or voids. (a3) Evaluation of the resilience of the healed sample. The sample could sustain a weight of 200 g. b-d) Representative stress versus strain curves for the composites before and after self-healing. e-f) The tensile strain (e) and stress (f) of the composites before and after healing.

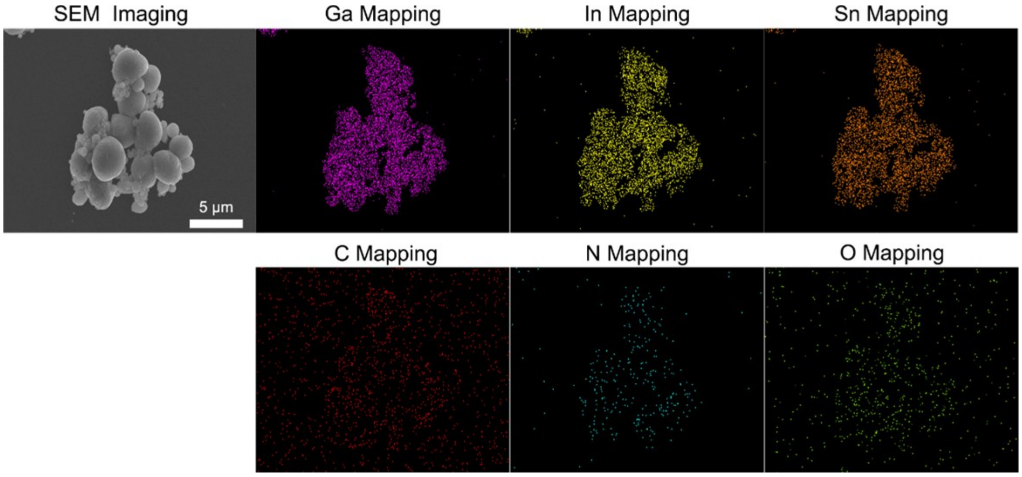

Fig. S14 SEM micrograph and EDS mapping of the LM droplets after removal of the macromolecules by washing with DMF. The presence of C, N, and O across the droplets demonstrates that the LM droplets were still encapsulated by a thin layer of polymer.

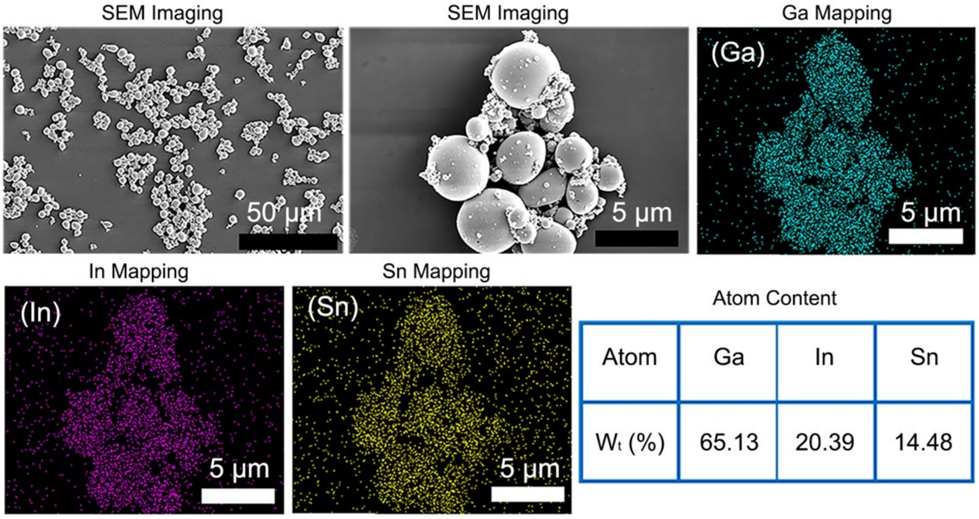

Atom	Ga	In	Sn
W$_t$ (%)	65.13	20.39	14.48

Fig. S15 SEM micrograph and EDS mapping of the recycled LM droplets.

According to the principle of recycling LM, the Ga content of the recycled liquid metal will decrease slightly. To prove this, we dispersed the recycled macroscopic LM droplet again and performed SEM and EDS measurement (Fig S15, ESI†). The results indicate that the proportion of the LM droplets is very close to that of the raw material (GaInSn (gallium (68.5%) − indium (21.5%) − tin (10%)).